1-1-2015

Luminescence-based chronologies for Palaeolithic sites in the Nihewan Basin, northern China: first tests using newly developed optical dating procedures for potassium feldspar grains

Yujie Guo
University of Wollongong, yg991@uowmail.edu.au

Bo Li
University of Wollongong, bli@uow.edu.au

Jia-Fu Zhang
Peking University

Richard G. Roberts
University of Wollongong, rgrob@uow.edu.au

Luminescence-based chronologies for Palaeolithic sites in the Nihewan Basin, northern China: first tests using newly developed optical dating procedures for potassium feldspar grains

Abstract

The Nihewan Basin in northern China is a key region in East Asia for the study of early human evolution, owing to the abundance of Palaeolithic sites with ages spanning the entire Pleistocene. However, most of the sites assigned to the Middle to Late Pleistocene have not been dated or are poorly dated, due to the lack of suitable numerical dating techniques. Optically stimulated luminescence (OSL) dating of quartz grains is commonly restricted to deposits younger than ~ 200 ka, but recent developments using the infrared stimulated luminescence (IRSL) emissions from grains of potassium-rich feldspar (K-feldspar) offer the potential to date Middle Pleistocene deposits using post-infrared IRSL (pIRIR) signals that do not suffer from 'anomalous fading'. In this paper, we report the first archaeological applications of the recently developed pre-dose multiple elevated temperature pIRIR (pMET-pIRIR) procedures for K-feldspar, which we applied to the sedimentary deposits at one Lower Palaeolithic site (Donggutuo) and one putatively Middle Palaeolithic site (Motianling) in the Nihewan Basin. Equivalent dose (De) values were measured, and non-fading signals were identified, using single-aliquot (SAR) and multiple-aliquot (MAR) regenerative-dose pMET-pIRIR procedures. For a sample from Donggutuo expected to be in field saturation, the natural pMET-pIRIR signals were consistent with, or close, to the laboratory saturation levels only when the MAR procedure was used. For the samples from Motianling, however, both the SAR and MAR procedures could be applied and these yielded indistinguishable De estimates. Our study shows that De values of up to 1500 Gy (or possibly 2000 Gy) can be measured using pMET-pIRIR procedures, corresponding to ages of up to 500 ka (or 650 ka) for deposits with environmental dose rates of ~ 3 Gy/ka, as is typical for this region. Our results also indicate that samples from a single study area (the Nihewan Basin) can respond differently to the same measurement conditions. As regards the archaeology of the Nihewan Basin, we date the upper part of the cultural layer at the Motianling site to 322 ± 33 ka and the underlying culturally sterile deposits to 370 ± 50 ka. These ages challenge the stratigraphic correlation of the stone artefacts to the Middle Palaeolithic and suggest that they should, instead, be assigned to the Lower Palaeolithic. Given this revised chronology, there is clearly a need to reassess the antiquity of other sites in the Nihewan Basin that have similarly been assigned previously to the Middle Palaeolithic. The pMET-pIRIR procedures tested in this paper show great promise as suitable chronometers for this task, and should be able to provide a timeline for human evolution and activities extending over the last half-million years in this key region of East Asia.

Disciplines

Medicine and Health Sciences | Social and Behavioral Sciences

Publication Details

Guo, Y., Li, B., Zhang, J. & Roberts, R. G. (2015). Luminescence-based chronologies for Palaeolithic sites in the Nihewan Basin, northern China: first tests using newly developed optical dating procedures for potassium feldspar grains. Journal of Archaeological Science: Reports, 3 31-40.

Luminescence-based chronologies for Palaeolithic sites in the Nihewan Basin, northern China: first tests using newly developed optical dating procedures for potassium feldspar grains

Yu-Jie Guo[1], Bo Li[1]*, Jia-Fu Zhang[2], Richard G. Roberts[1]

[1] *Centre for Archaeological Science, School of Earth and Environmental Sciences, University of Wollongong, Wollongong, NSW 2522, Australia*
[2] *MOE Laboratory for Earth Surface Processes, Department of Geography, College of Urban and Environmental Sciences, Peking University, Beijing 100871, China*

* *Corresponding author: bli@uow.edu.au*

Abstract

The Nihewan Basin in northern China is a key region in East Asia for the study of early human evolution, owing to the abundance of Palaeolithic sites with ages spanning the entire Pleistocene. However, most of the sites assigned to the Middle to Late Pleistocene have not been dated or are poorly dated, due to the lack of suitable numerical dating techniques. Optically stimulated luminescence (OSL) dating of quartz grains is commonly restricted to deposits younger than ~200 ka, but recent developments using the infrared stimulated luminescence (IRSL) emissions from grains of potassium-rich feldspar (K-feldspar) offer the potential to date Middle Pleistocene deposits using post-infrared IRSL (pIRIR) signals that do not suffer from 'anomalous fading'. In this paper, we report the first archaeological applications of the recently developed pre-dose multiple elevated temperature pIRIR (pMET-pIRIR) procedures for K-feldspar, which we applied to the sedimentary deposits at one Lower Palaeolithic site (Donggutuo) and one putatively Middle Palaeolithic site (Motianling) in the Nihewan Basin. Equivalent dose (D_e) values were measured, and non-fading signals were identified, using single-aliquot (SAR) and multiple-aliquot (MAR) regenerative-dose pMET-pIRIR procedures. For a sample from Donggutuo expected to be in field saturation, the natural pMET-pIRIR signals were consistent with, or close, to the laboratory saturation levels only when the MAR procedure was used. For the samples from Motianling, however, both the SAR and MAR procedures could be applied and these yielded indistinguishable D_e estimates. Our study shows that D_e values of up to 1500 Gy (or possibly 2000 Gy) can be measured using pMET-pIRIR procedures, corresponding to ages of up to 500 ka (or 650 ka) for deposits with environmental dose rates of ~3 Gy/ka, as is typical for this region. Our results also indicate that samples from a single study area (the Nihewan Basin) can respond differently to the same measurement conditions. As regards the archaeology of the Nihewan Basin, we date the upper part of the cultural layer at the Motianling site to 322 ± 33 ka and the underlying culturally sterile deposits to 370 ± 50 ka. These ages challenge the stratigraphic correlation of the stone artefacts to the Middle Palaeolithic and suggest that they should, instead, be assigned to the Lower Palaeolithic. Given this revised chronology, there is clearly a need to reassess the antiquity of other sites in the Nihewan Basin that have similarly been assigned previously to the Middle Palaeolithic. The pMET-pIRIR procedures tested in this paper show great promise as suitable chronometers for this task, and should be able to provide a timeline for human evolution and activities extending over the last half-million years in this key region of East Asia.

Key words: Nihewan Formation, Late Pleistocene, Middle Pleistocene, Middle Palaeolithic, Lower Palaeolithic, K-feldspar, infrared stimulated luminescence, IRSL, pMET-pIRIR, anomalous fading.

1. Introduction

The Nihewan Basin is located at the northeastern edge of the Chinese Loess Plateau, ~150 km west of Beijing, in Hebei and Shanxi Provinces (Fig. 1). It covers an area of ~ 9000 km^2 and contains thick lacustrine and fluvial sediments of the so-called Nihewan Formation (Yuan et al., 1996; Zhu et al., 2007). The Nihewan Formation and the overlying loess contain abundant mammalian fossils and lithic artefacts, making it one of the most important regions to study the palaeoenvironment, palaeontology and Palaeolithic archaeology of East Asia (Xie et al., 2006; Dennell, 2009, 2013). Over 100 Palaeolithic sites have been recorded in the Basin, and these have been assigned ages that span the entire Pleistocene, encompassing cultural phases extending from the Lower Palaeolithic to the Upper Palaeolithic (Xie et al., 2006).

Extensive chronological work has been conducted previously to constrain the ages of Early Pleistocene sites in the Basin, based on magnetostratigraphic dating (e.g., Zhu et al., 2004; Wang et al., 2005; Ao et al., 2013). Little work, however, has been done to date younger Pleistocene sites, mainly due to the lack of suitable dating techniques for these sites. Establishing a solid chronological framework for these sites is crucial not only for understanding the evolution of Palaeolithic cultures in East Asia, but also to help resolve long-standing debates about the presence or absence of the Middle Palaeolithic in East Asia (Gao, 1999, 2013; Gao and Norton, 2002; Norton et al., 2009; Yee, 2012; Li, 2014). At present, most of the 'Middle' and 'Late' Pleistocene sites in the Nihewan Basin have been classified as such based on the typology of the stone tools and on the stratigraphy of the cultural layers (Xie et al., 2006; Yuan et al., 2011), which are usually imprecise and sometimes controversial.

Radiocarbon (^{14}C) dating is applicable to plant and animal remains up to ~50 ka in age, but suitable organic materials are not always present at archaeological sites, even within this time range. Optical dating can be used to determine when mineral grains, such as quartz and potassium-rich feldspar (K-feldspar), were last exposed to sunlight (Huntley et al., 1985; Aitken, 1998; Roberts and Lian, 2015). The optically stimulated luminescence (OSL) emissions from quartz grains have been widely used to date the time of deposition of sediments at archaeological sites younger than ~200 ka (Lian and Roberts, 2006; Jacobs and Roberts, 2007; Wintle, 2008; Roberts et al., 2015), but there have been few applications to sediments in the Nihewan Basin using the quartz OSL signal (Shitaoka and Nagtomo, 2013; Nian et al., 2014). Zhao et al. (2010) investigated the potential of extending the age range beyond 200 ka using the recuperated OSL (ReOSL) signal from quartz grains extracted from the Nihewan Formation and overlying loess at the nearby (non-archaeological) Haojiatai section (Fig. 1). Their preliminary ages indicated that the Nihewan Formation was deposited before ~270 ka, followed by a hiatus before the loess began to accumulate at ~130 ka.

The infrared stimulated luminescence (IRSL) emissions from K-feldspar saturate at much higher radiation doses than does the conventional quartz OSL signal, so IRSL dating should be applicable to much older deposits if the problem of age underestimation associated with 'anomalous fading' (Wintle, 1973) can be corrected for appropriately (Huntley and Lamothe, 2001) or avoided altogether. Progress towards the latter goal has been achieved only recently with the development of post-infrared IRSL (pIRIR) procedures. These involve infrared stimulation as a two-step process (Thomsen et al., 2008) or at multiple elevated temperatures (Li and Li, 2011). The latter MET-pIRIR procedure enables non-fading signals to be isolated for dating, and Li and Li (2012) have shown that

equivalent dose (D_e) values of up to 1000 Gy can be measured reliably, corresponding to maximum ages of 300–500 ka at environmental dose rates of 2–3 Gy/ka. Li et al. (2013b, 2014a) extended this age range by more than half using a novel approach based on their observation that the sensitivity of the MET-pIRIR signal is dependent on the radiation dose received by the sample since burial. D_e values of up to ~1600 Gy could be measured using this newly developed 'pre-dose' MET-pIRIR (or pMET-pIRIR) procedure, thus bringing the entire Middle Pleistocene – and possibly the final stages of the Early Pleistocene – within dating range.

Although pIRIR and MET-pIRIR methods have been successfully tested on, and applied to, deposits throughout northern China (e.g., Li and Li, 2011, 2012; Buylaert et al., 2012; Fu et al., 2012; Gong et al., 2014), there have been no systematic investigations of the applicability of these procedures to sediments in the Nihewan Basin. Given the fact that the performance of pIRIR procedures is known to be sample dependent and can be affected by various measurement conditions (see recent review by Li et al., 2014b), it is important to test the suitability of these procedures for the samples of interest, and to characterise the luminescence behaviour of the dated K-feldspar grains, before attempting to determine the D_e values for age calculation.

In this paper, we report the test results for K-feldspars from two important archaeological sites in the Nihewan Basin (Fig. 1) that we have investigated using multiple-aliquot (MAR) and single-aliquot (SAR) regenerative-dose pMET-pIRIR procedures (Li et al., 2013b, 2014a). This is the first application of these novel procedures to archaeological deposits, so our main purpose here is to report the experimental data used to assess the suitability of the Nihewan Basin samples for pMET-pIRIR dating and to propose appropriate measurement procedures for a comprehensive dating program of Palaeolithic sites in the region.

2. Samples, experimental procedures and analytical facilities

Four samples taken from two Palaeolithic sites in the Nihewan Basin were selected for this initial study. One sample of lacustrine sediment, DGT-OSL-01, was taken from the cultural layer of the Donggutuo site (Fig. 2a). Its age is estimated to be ~1.1 Ma on the basis of magnetostratigraphic dating (Wang et al., 2005), so the K-feldspar grains should be in field saturation, provided the IRSL traps have not suffered from anomalous fading. Three additional samples (MTL-OSL-01, -07 and -10) were collected from the site of Motianling (Fig. 2b), which has tentatively been assigned to the Late Pleistocene, and the Middle Palaeolithic, based on stratigraphic correlations to the Hutouliang and Xishuidi sections in the Nihewan Basin (Xie et al., 2006). Sample MTL-OSL-01 was taken from the loess layer above the Nihewan Formation (about 50 cm above the loess-lacustrine boundary), whereas samples MTL-OSL-7 and -10 were taken from the lacustrine sediments below the loess deposits and within the Nihewan Formation. Sample MTL-OSL-07 is from the upper part of the cultural layer at Motianling, while sample MTL-OSL-10 is from the underlying culturally sterile deposits.

The samples were collected by hammering stainless steel tubes (5 cm in diameter) into the cleaned section faces. The tubes were removed and wrapped in light-proof plastic for transport to the Luminescence Dating Laboratory at the University of Wollongong. Additional bags of sediment were collected from the tube holes and sealed in zip-lock plastic bags for laboratory measurements of sample radioactivity and field water content. K-feldspar grains from each sample were extracted

following standard mineral separation techniques (Aitken, 1998). The samples were first treated using HCl acid and H_2O_2 solutions to eliminate carbonates and organic matter, respectively. K-feldspar grains of 63–90 μm or 63–106 μm were obtained by wet sieving and then density separation using a heavy liquid solution (2.58 g/cm^3). Finally the grains were etched in 10% HF acid for 10 min. K-feldspar grains covering the central ~5 mm diameter portion of each stainless steel disc were used for the IRSL measurements, corresponding to several hundreds of grains on each aliquot.

In optical dating, the depositional age of a sediment sample is calculated by dividing its D_e value (which is determined from measurements of luminescence signals) by the dose rate from environmental sources of ionising radiation (which are estimated separately). The environmental dose rate for HF etched grains consists of beta, gamma and cosmic radiation contributions external to the dated grains, and an internal beta dose rate from the radioactive decay of ^{40}K and ^{87}Rb inside the K-feldspar grains. The latter was estimated by assuming K and Rb concentrations of 13 ± 1% and 400 ± 100 ppm, respectively (Huntley and Baril, 1997; Huntley and Hancock, 2001; Zhao and Li, 2005; Li et al. 2008), and the cosmic-ray dose rate was estimated from the burial depth of each of the samples and the latitude, longitude and altitude of the two sites (Prescott and Hutton, 1994). To determine the external beta and gamma dose rates, we used a combination of low-level beta counting (Bøtter-Jensen and Mejdahl, 1988) and thick-source alpha counting (Aitken, 1985). Beta counting was used to directly measure the beta dose rate from ^{238}U, ^{235}U, ^{232}Th (and the daughter products in each series) and ^{40}K, and thick-source alpha counting was used to estimate the gamma dose rate from U, Th and their daughter products. The ^{40}K contribution to the gamma dose rate was obtained from the K content calculated from the beta and alpha counting data. Each of the external components of the total dose rate were adjusted for long-term sample water content, which was estimated as 10 ± 5% for the loess sample and 20 ± 5% for the three lacustrine samples, based on their measured (field) values. The dosimetry data for all samples are summarised in Table 1.

The IRSL measurements were performed on a Risø TL/OSL-DA-20 reader equipped with a ^{90}Sr/^{90}Y beta source and infrared diodes for stimulation (870 Δ 40 nm). The beta dose delivered to the grains was calibrated using grains of 90–125 and 180–212 μm diameter, but it has been shown previously that the delivered dose is the same for grains as small as 40–55 μm in diameter (Armitage and Bailey, 2005; Goedicke, 2007). IRSL signals were detected by an Electron Tubes Ltd 9235B photomultiplier tube fitted with Schott BG-39 and Corning 7-59 filters, which transmit blue (320–480 nm) light. For the pMET-pIRIR measurements, infrared stimulation was performed successively at six temperatures (50, 100, 150, 200, 250 and 280 °C). The stimulation at 280 °C is higher than that used in the original pMET-pIRIR procedure, but we show below that it is needed to isolate a non-fading signal for the field-saturated Donggutuo sample. To monitor and minimise interference from isothermal decay signals, aliquots were held for 10, 10, 20, 20, 30 and 50 s before the infrared stimulations at 50, 100, 150, 200, 250 and 280 °C, respectively (following Fu et al., 2012). Test doses of 51 Gy were given in this study, except in the fading test on sample MTL-OSL-07 (when a test dose of 24 Gy was used). A preheat at 320 °C for 60 s was applied to each of the natural, regenerative and test doses before the infrared stimulations, which were made for 100 s. The D_e value for each aliquot was calculated from the IRSL counts integrated over the first 10 s of IRSL decay, minus the counts from the final 10 s of stimulation as background. The SAR and MAR procedures used in this study are summarised in Tables 2 and 3, respectively. For the SAR procedure, 4–10 aliquots were used to

determine the final D_e value of each sample (Table 1). A solar simulator (Dr Hönle UVACUBE 400) was used to give the 2 hr bleach at step 17 of the SAR procedure.

3. SAR and MAR pMET-pIRIR tests on sample DGT-OSL-01

We first tested the stability of the pMET-pIRIR signals using sample DGT-OSL-01. The natural dose of this sample is expected to be ~3100 Gy, based on its expected age of ~1.1 Ma (Wang et al., 2005) and measured environmental dose rate of 2.80 Gy/ka (Table 1). Such a high natural dose would have saturated the corresponding IRSL traps, provided no fading has occurred. Hence, the natural intensity of any non-fading IRSL signal should be consistent with the saturation level of the laboratory dose response curve (DRC).

3.1 SAR pMET-pIRIR procedure

We first applied the SAR pMET-pIRIR procedure of Li et al. (2014a) to sample DGT-OSL-01, following the experimental steps listed in Table 2. This procedure is based on the recent discovery of a strong dose dependence of the MET-pIRIR signal sensitivity (Li et al., 2013b). The 'sensitivity' can be monitored using the pIRIR signal induced by stimulation of a test dose given in the natural dose cycle (T_n) and each regenerative-dose cycle (T_x). Li et al. (2013b) found that incorporating a solar simulator bleach for 2 hr at the end of each SAR cycle can reset the pre-dose 'memory' from the preceding cycle. As a result, there is no need to correct for sensitivity changes, and Li et al. (2014a) suggested that the sensitivity-corrected (L_x/T_x), test dose (T_x) and sensitivity-uncorrected (L_x) pMET-pIRIR signals can be used for D_e estimation. They found that both the T_x and L_x signals saturate at a higher dose than the L_x/T_x signal, thereby extending the age limit beyond the range of conventional pIRIR methods.

Four aliquots were measured using the SAR pMET-pIRIR procedure. The DRCs of the different pMET-pIRIR signals are shown in Fig. 3. For all four aliquots, recycling ratios of between 0.95 and 1.05 were obtained for the L_x/T_x, L_x and T_x signals, indicating that sensitivity change in the regenerative-dose L_x signals is appropriately monitored using the T_x signals, and that any pre-dose dependency of the sensitivity was fully reset using the 2 hr solar simulator bleach at the end of each SAR cycle. The sensitivity-corrected natural signal (L_n/T_n) measured at 280 °C reaches 93.5 ± 2.5 % of the saturation level of the DRC (Fig. 3a), which is close to the saturation value expected for this sample. In contrast, the signals for the natural dose (L_n) and its corresponding test dose (T_n) lie more than 10% away from saturation – that is, less than 89% of the saturation level of their respective DRCs – even for the pMET-pIRIR signals measured at high temperatures (>200 °C). There are several possible explanations for these results: 1) L_x has a higher proportion of dose-dependent unbleachable signal than L_n (Li et al., 2013a); 2) the natural dose suffers from anomalous fading, so L_n lies below the saturation level of the laboratory DRC; 3) a significant sensitivity change occurred during the measurement of L_n, so that the luminescence efficiency differed between stimulation of the natural dose and the subsequent regenerative doses; or 4) some combination of these possibilities.

The first possibility can be tested by applying an 'intensity-subtraction' procedure to correct for any unbleachable signal (Li et al. 2013a). To do this, three natural aliquots were bleached for 10 hr using the solar stimulator and the remaining unbleachable or 'residual' L_n signals were then measured. After this, the same aliquots were given a series of regenerative doses, and each of the

aliquots was then bleached for 2 hr in the solar stimulator prior to pMET-pIRIR measurements to obtain the corresponding residual L_x signals. The residual pMET-pIRIR signals measured at 280 °C for the natural and regenerative doses are shown in Fig. 4, which reveals similar proportions of unbleachable (residual) signals in L_n and L_x, and T_n and T_x; the values for L_n and T_n are plotted on the *y*-axis. The residual signals account for about 13%, 5% and 40% of the respective L_x/T_x, L_x and T_x signals in Fig. 3, which suggests that the underestimation of L_n relative to the saturation level of the laboratory DRC is not due to a dose-dependent residual. Similar observations were obtained for the pMET-pIRIR signals measured at lower temperatures, but the latter unbleachable (residual) signals account for a much smaller proportion of the pMET-pIRIR signals than do those measured at 280 °C.

The second and third possible explanations mentioned above were tested using a dose recovery test (Galbraith et al., 1999; Wallinga et al., 2000), because any effects of anomalous fading can be avoided in this laboratory-based test. Four aliquots of DGT-OSL-01 were first bleached for 4 hr using the solar simulator, and then given a dose of 1047 Gy as a surrogate 'natural' dose. The aliquots were then measured using the SAR pMET-pIRIR procedure in Table 2. The ratios of the measured (recovered) to given doses are shown in Fig. 5 for the various pMET-pIRIR signals. The L_x/T_x signals measured at 100–280 °C yielded dose recovery ratios consistent with unity, although with large uncertainties because the given dose is close to the saturation region. For the L_x and T_x signals, however, the dose recovery ratios were significantly less than unity at all stimulation temperatures, which suggests that the SAR pMET-pIRIR procedure is suitable for this sample only when the sensitivity-corrected signal (L_x/T_x) is used. The fact that the dose recovery ratios obtained from the L_x and T_x signals were too small indicates that a significant sensitivity change occurred during the measurement of the natural signal, or that the pre-dose dependency of the natural signal differs from that of the regenerated signals.

3.2 MAR pMET-pIRIR procedure

To avoid the problem caused by sensitivity change during measurement of the natural signal, and any possible cumulative sensitivity change induced by the successive dose and measurement cycles in the SAR procedure, we tested the multiple-aliquot version of the pMET-pIRIR procedure (Li et al., 2013b). This involves only one cycle of measurements for each aliquot. The experimental steps employed in the MAR procedure are summarised in Table 3. These are the same as those proposed originally by Li et al. (2013b), except for the incorporation of an additional infrared stimulation at 280 °C (steps 8, 16 and 25) and the heating of the aliquots to 500 °C (instead of 600 °C) at step 17.

Aliquots were divided into 7 separate groups: one group was used to measure the natural signals and the other 6 groups were bleached in the solar simulator for several hours before receiving different regenerative doses. The L_n and L_x signals, and the corresponding test dose signals (T_1) were then measured (steps 3–8 and 11–16), after which the aliquots were heated to 500 °C before another test dose was applied and the corresponding signals (T_2) were measured (steps 20–25). Li et al. (2013b) demonstrated that T_1 is dependent on the pre-dose received, but T_2 is not. They suggested, therefore, that the T_2 signals could be used to normalise each of the aliquots for inter-aliquot variation, which is a key requirement for precise D_e determination using any multiple-aliquot procedure. D_e values can then be estimated from the sensitivity-corrected L_n/T_1 and L_x/T_1 signals, and the inter-aliquot normalised L_n/T_2, L_x/T_2 and T_1/T_2 signals.

The multiple-aliquot DRCs for the pMET-pIRIR signals are shown in Fig. 6. All natural signals measured at 280 °C are close to, or consistent with, the saturation levels of the DRCs, reaching 90.8 ± 4.7%, 93.2 ± 7.6% and 106.7 ± 10.0% of the saturation intensities of the L_n/T_1, L_n/T_2, and T_n/T_2 signals, respectively. This result indicates that these signals are stable and fade negligibly, so we suggest that the MAR pMET-pIRIR procedure is more suitable than the SAR counterpart for dating old samples from the Nihewan Basin. We cannot produce a finite age for sample DGT-OSL-01 because it is in field saturation, but a minimum depositional age of ~700 ka is obtained from the saturation dose of ~2000 Gy for the MAR L_x/T_2 signal measured at 280 °C (Fig. 6b), divided by the environmental dose rate of 2.80 Gy/ka.

4. SAR and MAR pMET-pIRIR tests on samples from Motianling

The SAR and MAR procedures were also tested on the three samples from the Motianling site, which were expected to lie within the applicable range of pMET-pIRIR methods.

We first checked the performance of the SAR pMET-pIRIR procedure on sample MTL-OSL-07, which was collected from the upper part of the cultural layer at this site, using a dose recovery test. The same measurement procedure was used as described above for sample DGT-OSL-01, except that a smaller given dose (960 Gy) was applied. The dose recovery ratios for the various signals are shown in Fig. 7. All of the signals stimulated at temperatures above 150 °C yielded ratios consistent with unity, which demonstrates that a known laboratory dose can be accurately recovered for this sample using the single-aliquot pMET-pIRIR procedure. Unlike the Donggutuo sample, the L_x and T_x signals did not give ratios much smaller than unity, indicating that the sensitivities of the natural and regenerated signals are similar and that the pre-dose dependency of the sensitivity was successfully reset using a 2 hr solar simulator bleach at the end of each SAR cycle.

We also conducted a laboratory fading test on sample MTL-OSL-07 to check that the high-temperature pMET-pIRIR signals faded negligibly. Four aliquots that had been used for D_e measurements (using the SAR pMET-pIRIR procedure) were given an infrared bleach at 320 °C (to ensure that the infrared-sensitive traps were empty) and fading measurements were then performed using a conventional single-aliquot MET-pIRIR procedure (following Li and Li, 2011) and regenerative and test doses of 80 Gy and 24 Gy, respectively. After the bleached aliquots had received a regenerative dose and been preheated, they were stored for periods of up to 6 days at room temperature before MET-pIRIR measurements. For practical reasons, an infrared bleach at 320 °C for 100 s, rather than a solar simulator bleach for 2 hr, was given at the end of each SAR cycle to minimise the size of any residual signals. The normalised MET-pIRIR L_x/T_x signals are plotted against storage time in Fig. 8a, and the corresponding fading rates are displayed in Fig. 8b. These data show that the fading rate is highest when the IRSL signal is measured at 50 °C (2.7 ± 0.1%/decade) and decreases steadily as the temperature is raised, as has been commonly reported (see Li et al., 2014b). Fading rates of less than 1%/decade are observed at stimulation temperatures of 250 and 280 °C, supporting the inferred negligible fading rate of the MET-pIRIR 280 °C signal in the field-saturated sample from Donggutuo.

Fig. 9 shows the D_e values obtained from the various SAR and MAR pMET-pIRIR signals for all three Motianling samples, plotted as a function of stimulation temperature. For each sample, a plateau in D_e values is obtained at pMET-pIRIR stimulation temperatures above 200 °C, indicating the

existence of non-fading signals at these elevated temperatures. For the loess sample (MTL-OSL-01), the SAR L_x/T_x, L_x and T_x signals measured at 280 °C give statistically consistent D_e values (349 ± 36, 357 ± 53 and 319 ± 65 Gy, respectively), while the MAR L_x/T_1, L_x/T_2 and T_1/T_2 signals measured at 280 °C also yield statistically consistent, but slightly smaller, D_e values (319 ± 49, 301 ± 20 and 295 ± 31 Gy, respectively). For the sample collected from deposits underlying the cultural layer at this site (MTL-OSL-10), the D_e values for the various SAR and MAR signals measured at 280 °C are statistically compatible at 1σ and range from about 900 Gy to 1500 Gy (Fig. 9c). These results confirm that both the SAR and MAR pMET-pIRIR procedures are suitable for dating K-feldspars at Motianling. Based on these findings, sample MTL-OSL-07 was measured using only the SAR procedure and the highest stimulation temperature applied was 250 °C (Fig. 9b). For the latter signals, we obtained statistically concordant D_e values of 925 ± 51 Gy (L_x/T_x), 994 ± 97 Gy (L_x) and 987 ± 205 Gy (T_x).

To estimate the final D_e values and ages for the Motianling samples (Table 1), we used the weighted mean of the D_e values calculated from the SAR L_x and MAR L_x/T_2 signals measured at the highest stimulation temperatures – namely, 280 °C for samples MTL-OSL-01 and -10, and 250 °C for sample MTL-OSL-07. The ages obtained for the three samples are in correct stratigraphic order, increasing from 102 ± 7 ka for the capping loess deposits, to 322 ± 33 ka for the upper part of the artefact-bearing layer at this site, and 370 ± 50 ka for the underlying lacustrine deposits. The artefacts from this site have previously been attributed to the Middle Palaeolithic, based on stratigraphic correlations between sites in the Nihewan Basin (Xie et al., 2006). However, the pMET-pIRIR ages of more than 300 ka (or 256 ka at 2σ) obtained in this study for the relevant samples from the Nihewan Formation are much older than the commonly accepted time span for the Chinese 'Middle Palaeolithic', from about 140 to 30 ka ago (Gao and Norton, 2002), which implies that Motianling might be a Lower Palaeolithic site. These findings demonstrate the need to reassess the numerical chronology of other sites in the region that have been classified as Middle Palaeolithic based on stratigraphic correlations.

Finally, we note that the pMET-pIRIR ages for K-feldspars at Motianling are consistent with the ReOSL ages reported by Zhao et al. (2010) for quartz grains collected from the nearby Haojiatai section (Fig. 1). Their ReOSL age of ~130 ka for the start of loess accumulation is similar to our pMET-pIRIR age of ~110 ka for loess sample MTL-OSL-01, and their quartz-based timeframe for deposition of the Nihewan Formation before ~270 ka is compatible with our K-feldspar ages of more than 300 ka. Like Zhao et al. (2010), we observe a prolonged gap (>140 ka) in sedimentation between the lacustrine and overlying loess deposits, which at Motianling extends over two entire glacial cycles, from Marine Isotope Stage (MIS) 9 to the last interglacial (MIS 5). Without additional numerical ages, we cannot say if this hiatus is widespread throughout the Nihewan Basin, but the search for Middle Palaeolithic sites may prove challenging if deposits dating to between 250 and 130 ka are scarce.

5. Considerations for chronology-building in the Nihewan Basin

One of the main benefits claimed for pIRIR dating procedures is that a non-fading signal can be measured for K-feldspar, and the latter can be tested in several ways. First, laboratory fading tests can be conducted (Huntley and Lamothe, 2001) and these should indicate negligible rates of fading, at least on laboratory timescales (Fig. 8). Second, a plateau of D_e values as a function of infrared stimulation temperature should be observed using multiple elevated temperature pIRIR procedures (Fig. 9), provided the K-feldspar grains were sufficiently bleached prior to deposition. Third, an

infinitely old (or field saturated) sample can be measured in order to check that the intensity of the natural signal is consistent with the saturation level of the regenerated DRC in the laboratory; the latter implies that a non-fading signal is present (Fig. 6).

In this study, we have demonstrated that a natural signal that falls below the laboratory saturation level does not necessarily mean that this signal has faded, but that other reasons, such as sensitivity change or inappropriate sensitivity correction, may also need to be considered. This was the case with the L_n and T_n signals for the Donggutuo sample, when measured using the SAR pMET-pIRIR procedure (Fig. 3b and 3c). The expected age of this sample is ~1.1 Ma, so the IRSL traps should have been saturated in the natural sample. We attribute the substantial underestimation of the natural intensities relative to the saturation level of the regenerated DRC to a significant sensitivity change during measurement of the natural signal. Our interpretation is supported by the observation that the MAR pMET-pIRIR procedure improved the match between the natural and DRC saturation intensities of the L_x and T_x signals for the same sample (Fig. 6b and 6c).

The Motianling samples exhibited no underestimation of the natural signal using the SAR pMET-pIRIR procedure, which implies that the pre-dose dependency of the sensitivity was successfully reset using a 2 hr solar simulator bleach at the end of each SAR cycle. This suggestion is supported by the similarity in shape of the SAR and MAR dose response curves for the three samples (DGT-OSL-01, MTL-OSL-01 and -10) measured using both procedures, because the DRCs would be expected to differ in shape if there were cumulative sensitivity changes between each of the SAR cycles. For these three samples, Fig. 10 shows the regenerative-dose sensitivity-corrected signals (L_x/T_x or L_x/T_1), sensitivity-uncorrected signals (L_x or L_x/T_2) and test dose signals (T_x or T_1/T_2) stimulated at 280 °C using the SAR or MAR procedures. In each case, the samples exhibit similar SAR and MAR dose response trends, thus implying that a sensitivity change during measurement of the natural signal is responsible for the underestimation of the L_n and T_n signals for the Donggutuo sample, rather than cumulative sensitivity changes in the subsequent SAR cycles. We have also demonstrated that this problem may be overcome by applying a MAR procedure, in which only the data from the first SAR cycle of each aliquot are used for D_e determination.

The DRC data shown in Fig. 10 can be fitted using a single saturating exponential function, which yields characteristic saturation dose (D_0) values of about 370, 660 and 550 Gy for L_x/T_x (or L_x/T_1), L_x (or L_x/T_2) and T_x (or T_1/T_2), respectively. If a $2.3D_0$ value is taken as a conservative upper limit of reliable D_e estimation (corresponding to 90% of the saturation value), it is possible to estimate D_e values as high as 1500 Gy from the sensitivity-uncorrected signal (L_x or L_x/T_2) measured using pMET-pIRIR procedures. This corresponds to an age of ~500 ka for a dose rate of 3 Gy/ka, which is typical of the sediments in the Nihewan Basin. At $3D_0$, which corresponds to 95% of the saturation intensity, the corresponding limits are 2000 Gy and ~650 ka.

SAR and MAR procedures each have advantages and disadvantages (see Li et al., 2014a for detailed discussion), so if one procedure is not suited to a particular circumstance or sample, then the other may be. We have shown that the MAR procedure is more suitable than the SAR procedure for the ~1.1 Ma sample from Donggutuo, but that the SAR and MAR procedures yield indistinguishable results for the 100–400 ka samples from Motianling. Our results indicate that samples from different sites in the Nihewan Basin can behave differently to identical pIRIR procedures, depending on their depositional age and/or the source and pre-burial history of the K-

feldspar grains. To obtain reliable ages for other sites in the Basin and elsewhere, we recommend that the SAR pMET-pIRIR procedure is adopted initially and that the MAR pMET-pIRIR procedure should be applied to samples that fail the SAR dose recovery test.

6. Conclusions

Newly developed IRSL dating techniques hold great promise for dating sediments from archaeological sites in the Nihewan Basin and in other regions where K-feldspars have suitable physical properties. In this study, we have described the first archaeological application of the recently reported pMET-pIRIR procedures for K-feldspar and shown that non-fading signals can be identified using single- and multiple-aliquot D_e measurement procedures. We recognise, however, that samples collected from different sites may behave differently, so we recommend further testing of these new procedures at each site investigated. We found it essential to perform a dose recovery test before routinely applying the SAR procedure and, for samples that fail this test, the MAR procedure may provide an alternative method of measuring the D_e.

For the Motianling site, our data indicate that that the cultural layer was deposited 322 ± 33 ka ago. This shows either that the Middle Palaeolithic is older than previously thought, or that it should be reclassed as Lower Palaeolithic. Further numerical dating studies will reveal the true antiquity of Palaeolithic deposits in the Nihewan Basin. Based on the data collected in this study, pMET-pIRIR procedures should be capable of providing reliable estimates of D_e of up to 1500–2000 Gy, equating to a dating limit of 500–650 ka for deposits in this region. Given this extended timeframe, the last half-million years of human activities and evolution in the Nihewan region can now be considered to lie within range of optical dating, encompassing the Holocene, the Late Pleistocene and much of the Middle Pleistocene.

Acknowledgements

This study was supported by postgraduate scholarships from the China Scholarship Council and the University of Wollongong to Y.G., a University of Wollongong Vice-Chancellor's Postdoctoral Research Fellowship to B.L., the National Natural Science Foundation of China to J.Z. (NSFC, No. 41171007), and an Australian Research Council Australian Laureate Fellowship to R.G.R. (FL130100116). We thank Baoyin Yuan, Weiwen Huang, Yue Hu, Yongmin Meng, Qi Wei, Shengquan Cheng, Fagang Wang, Fei Xie and others who helped with the field investigations and sample collection, and the two reviewers for their valuable and constructive comments.

References

Aitken, M.J., 1985. Thermoluminescence Dating. Academic Press, London.

Aitken, M.J., 1998. An Introduction to Optical Dating. Oxford University Press, Oxford.

Ao, H., Deng, C., Dekkers, M.J., Liu, Q., 2010. Magnetic mineral dissolution in Pleistocene fluvio-lacustrine sediments, Nihewan Basin (North China). Earth and Planetary Science Letters 292, 191–200.

Ao, H., Dekkers, M.J., Wei, Q., Qiang, X., Xiao, G., 2013. New evidence for early presence of hominids in North China. Scientific Reports 3, 2403.

Armitage, S.J., Bailey, R.M., 2005. The measured dependence of laboratory beta dose rates on sample grain size. Radiation Measurements 39, 123–127.

Bøtter-Jensen, L., Mejdahl, V., 1988. Assessment of beta dose rate using a GM multicounter system Nuclear Tracks and Radiation Measurements 14, 187–191.

Buylaert, J.-P., Jain, M., Murray, A. S., Thomsen, K. J., Thiel, C., Sohbati, R., 2012. A robust feldspar luminescence dating method for Middle and Late Pleistocene sediments. Boreas 41, 435–451.

Dennell, R.W., 2009. The Palaeolithic Settlement of Asia. Cambridge University Press, Cambridge.

Dennell, R.W., 2013. The Nihewan Basin of North China in the Early Pleistocene: Continuous and flourishing, or discontinuous, infrequent and ephemeral occupation? Quaternary International 295, 223–236.

Fu, X., Li, B., Li, S.H., 2012. Testing a multi-step post-IR IRSL dating method using polymineral fine grains from Chinese loess. Quaternary Geochronology 10, 8–15.

Galbraith, R.F., Roberts, R.G., Laslett, G.M., Yoshida, H., Olley, J.M., 1999. Optical dating of single and multiple grains of quartz from Jinmium rock shelter, northern Australia: Part I, experimental design and statistical models. Archaeometry 41, 339–364.

Gao, X., 1999. A discussion of the 'Chinese Middle Paleolithic.' Acta Anthropologica Sinica 18, 1–16 (in Chinese).

Gao, X., 2013. Paleolithic cultures in China: uniqueness and divergence. Current Anthropology 54, Supplement 8, S358–S370.

Gao, X., Norton, C.J., 2002. A critique of the Chinese 'Middle Palaeolithic'. Antiquity 76, 397–412.

Goedicke, C., 2007. Calibration of a $^{90}Sr/^{90}Y$-source for luminescence dating using OSL. Radiation Measurements 42, 1427–1431.

Gong, Z.J., Li, S.H., Li, B., 2014. The evolution of a terrace sequence along the Manas River in the northern foreland basin of Tian Shan, China, as inferred from optical dating. Geomorphology 213, 201–212.

Huntley, D.J., Baril, M.R., 1997. The K content of the K-feldspars being measured in optical dating or in thermoluminescence dating. Ancient TL 15, 11–13.

Huntley, D.J., Hancock, R.G.V., 2001. The Rb contents of the K-feldspars being measured in optical dating. Ancient TL 19, 43–46.

Huntley, D.J., Lamothe, M., 2001. Ubiquity of anomalous fading in K-feldspars and the measurement and correction for it in optical dating. Canadian Journal of Earth Sciences 38, 1093–1106.

475 Huntley, D.J., Godfrey-Smith, D.I., Thewalt, M.L.W., 1985. Optical dating of sediments. Nature 313,
476 105–107.

477 Jacobs, Z., Roberts, R.G., 2007. Advances in optically stimulated luminescence dating of individual
478 grains of quartz from archeological deposits. Evolutionary Anthropology 16, 210–223.

479 Li, B., Li, S.H., 2011. Luminescence dating of K-feldspar from sediments: a protocol without
480 anomalous fading correction. Quaternary Geochronology 6, 468–479.

481 Li, B., Li, S.H., 2012. Luminescence dating of Chinese loess beyond 130 ka using the non-fading signal
482 from K-feldspar. Quaternary Geochronology 10, 24–31.

483 Li, B., Li, S.H., Wintle, A.G., Zhao, H., 2008. Isochron dating of sediments using luminescence of K-
484 feldspar grains. Journal of Geophysical Research–Earth Surface 113, F02026.

485 Li, B., Roberts, R.G., Jacobs, 2013a. On the dose dependency of the bleachable and non-bleachable
486 components of IRSL from K-feldspar: improved procedures for luminescence dating of
487 Quaternary sediments. Quaternary Geochronology 17, 1–13.

488 Li, B., Jacobs, Z., Roberts, R.G., Li, S.H., 2013b. Extending the age limit of luminescence dating using
489 the dose-dependent sensitivity of MET-pIRIR signals from K-feldspar. Quaternary
490 Geochronology 17, 55–67.

491 Li, B., Roberts, R.G., Jacobs, Z., Li, S.H., 2014a. A single-aliquot luminescence dating procedure for K-
492 feldspar based on the dose-dependent MET-pIRIR signal sensitivity. Quaternary
493 Geochronology 20, 51–64.

494 Li, B., Jacobs, Z., Roberts, R.G., Li, S.H., 2014b. Review and assessment of the potential of post-IR IRSL
495 dating methods to circumvent the problem of anomalous fading in feldspar luminescence.
496 Geochronometria 41, 178–201.

497 Li, F., 2014. Fact or fiction: the Middle Palaeolithic in China. Antiquity 88, 1303–1309.

498 Lian, O.B., Roberts, R.G., 2006. Dating the Quaternary: progress in luminescence dating of
499 sediments. Quaternary Science Reviews 25, 2449–2468.

500 Nian, X.M., Gao, X., Xie, F., Mei, H.J., Zhou, L.P., 2014. Chronology of the Youfang site and its
501 implications for the emergence of microblade technology in North China. Quaternary
502 International 347, 113–121.

503 Norton, C.J., Gao, X., Feng, X.W., 2009. The East Asian Middle Palaeolithic reexamined. In Camps, M.
504 and Chauhan, P. (Eds), Sourcebook of Paleolithic Transition, pp. 245–254. Springer, Dordrecht.

505 Prescott, J.R., Hutton, J.T., 1994. Cosmic ray contributions to dose rates for luminescence and ESR
506 dating: large depths and long-term time variations. Radiation Measurements 23, 497–500.

507 Roberts, R.G., Lian, O.B., 2015. Illuminating the past. Nature 520, 438–439.

508 Roberts, R.G., Jacobs, Z., Li, B., Jankowski, N.R., Cunningham, A.C., Rosenfeld, A.B., 2015. Optical
509 dating in archaeology: thirty years in retrospect and grand challenges for the future. Journal of
510 Archaeological Science 56, 41–60.

511 Shitaoka, Y., Nagatomo, T., 2013. OSL dating using quartz fine grains extracted from loess in Upper
512 Palaeolithic sites of Nihewan Basin, northern China. Geochronometria 40, 311–316.

513 Thomsen, K.J., Murray, A.S., Jain, M., Bøtter-Jensen, L., 2008. Laboratory fading rates of various
514 luminescence signals from feldspar-rich sediment extracts. Radiation Measurements 43,
515 1474–1486.

516 Wallinga, J., Murray, A., Wintle, A., 2000. The single-aliquot regenerative-dose (SAR) protocol
517 applied to coarse-grain feldspar. Radiation Measurements 32, 529–533.

518 Wang, H., Deng, C., Zhu, R., Wei, Q., Hou, Y., Boëda, E., 2005. Magnetostratigraphic dating of the
519 Donggutuo and Maliang Paleolithic sites in the Nihewan Basin, North China. Quaternary
520 Research 64, 1–11.

521 Wei, Q., 2004. The Paleolithic of Nihewan Basin. In: Lu, Z.E. (Ed.), Review of China's Century of
522 Archaeological Research (Paleolithic Archaeology), pp. 84–110. Beijing Science Press, Beijing.

523 Wintle, A.G., 1973. Anomalous fading of thermoluminescence in mineral samples. Nature 245, 143–
524 144.

525 Wintle, A.G., 2008. Luminescence dating: where it has been and where it is going. Boreas 37, 471–
526 482.

527 Xie, F., Li, J., Liu, L.Q., 2006. Paleolithic Archeology in the Nihewan Basin. Huashan Literature and
528 Arts Press, Shijiazhuang (in Chinese).

529 Yee, M.K., 2012. The Middle Palaeolithic in China: a review of current interpretations. Antiquity 86,
530 619–626.

531 Yuan, B.Y., Zhu, R.X., Tian, W.L., Cui, J.X., Li, R.Q., Wang, Q., Yan, F.H., 1996. Magnetostratigraphic
532 dating on the Nihewan Formation. Science in China (Series D) 26, 67–73 (in Chinese).

533 Yuan, B.Y., Xia, Z.K., Niu, P.S. (Eds), 2011. Nihewan Rift and Early Man. Geology Press, Beijing (in
534 Chinese).

535 Zhao, H., Li, S.H., 2005. Internal dose rate to K-feldspar grains from radioactive elements other than
536 potassium. Radiation Measurements 40, 84–93.

537 Zhao, H., Lu, Y., Wang, C., Chen, J., Liu, J., Mao, H., 2010. ReOSL dating and fluvial sediments from
538 Nihewan Basin, northern China and its environmental application. Quaternary Geochronology
539 5, 159–163.

540 Zhu, R.X., Potts, R., Xie, F., Hoffman, K.A., Deng, C.L., Shi, C.D., Pan, Y.X., Wang, H.Q., Shi, R.P., Wang,
541 Y.C., Shi, G.H., Wu, N.Q., 2004. New evidence on the earliest human presence at high northern
542 latitudes in northeast Asia. Nature 431, 559–562.

543 Zhu, R.X., Deng, C.L., Pan, Y.X., 2007. Magnetochronology of the fluvio-lacustrine sequences in the
544 Nihewan Basin and implications for early human colonization of northeast Asia. Quaternary
545 Sciences 27, 922–944 (in Chinese with English abstract).

546

Figure captions

Fig. 1: Maps showing the Nihewan Basin and the locations of the two study sites (Donggutuo and Motianling). The Haojiatai section studied by Zhao et al. (2010) is also shown. Modified from Wei (2004) and Ao et al. (2010).

Fig. 2: Photos showing the sampling locations (red stars) at (a) Donggutuo and (b) Motianling. The black stippled line in (b) demarcates the contact between the Nihewan Formation and the overlying loess deposits. The Donggutuo sample is located 6.3 m below ground surface, while the people standing next to archaeological sample MTL-OSL-07 provide an approximate scale in (b).

Fig. 3: Dose response curves for the (a) L_x/T_x, (b) L_x and (c) T_x signals measured at different stimulation temperatures using the SAR pMET-pIRIR procedure for sample DGT-OSL-01. The natural signals are shown as the upper set of data points on the *y*-axis. The horizontal dashed lines represent the intensities of the natural signals for the 280 °C signals. Each data point represents the mean value for four aliquots and the corresponding standard errors are smaller than the size of the symbols. The curves were fitted using a single saturating exponential function of the form $I = I_0*(1–e^{-D/D_0}) + y$, where I is the normalised IRSL intensity, D is the regenerative dose, D_0 is the characteristic saturation dose, and the sum of I_0 and y is the saturation value of the exponential curve, and were then normalised to unity at a dose of 766 Gy.

Fig. 4: Residual (unbleachable) signals measured for sample DGT-OSL-01 at an infrared stimulation temperature of 280 °C using the SAR pMET-pIRIR procedure. The natural residual signals (L_n/T_n, L_n and T_n) are shown by open symbols on the *y*-axis. Each data point represents the mean value for three aliquots and the corresponding standard errors are smaller than the size of the symbols.

Fig. 5: Dose recovery ratios (measured to given dose) for the L_x/T_x, L_x and T_x signals of sample DGT-OSL-01, plotted against the SAR pMET-pIRIR stimulation temperature. Each data point represents the mean value for four aliquots and the vertical bars indicate the corresponding standard errors. For clarity, the data points for L_x and T_x are offset laterally at each stimulation temperature.

Fig. 6: Dose response curves for the (a) L_x/T_1, (b) L_x/T_2 and (c) T_1/T_2 signals measured at different stimulation temperatures using the MAR pMET-pIRIR procedure for sample DGT-OSL-01. The natural signals are shown as the upper set of data points on the *y*-axis. Each data point represents the mean value for 4–6 separate aliquots and the vertical bars indicate the corresponding standard errors. The curves were fitted using a single saturating exponential function (see Fig. 3 caption) and normalised to unity at a dose of 800 Gy.

Fig. 7: Dose recovery ratios for the L_x/T_x, L_x and T_x signals of sample MTL-OSL-07, plotted against the SAR pMET-pIRIR stimulation temperature. Each data point represents the mean value for four aliquots and the vertical bars indicate the corresponding standard errors. For clarity, the data points for L_x and T_x are offset laterally at each stimulation temperature.

Fig. 8: (a) Decay of the L_x/T_x signals from sample MTL-OSL-07 measured at different stimulation temperatures using the SAR MET-pIRIR procedure and plotted as a function of storage time, t. The signals were normalised to the time between irradiation and first measurement, t_c (705, 855, 1031, 1228, 1442 and 1678 s for the signals measured at 50, 100, 150, 200, 250 and 280 °C, respectively).

(b) Anomalous fading rates (g-values, expressed in % per decade) for the MET-pIRIR signals, based on the data in (a). See Aitken (1985) and Huntley and Lamothe (2001) for discussion of fading models.

Fig. 9: D_e values for samples (a) MTL-OSL-01, (b) MTL-OSL-07 and (c) MTL-OSL-10 measured at different stimulation temperatures using the SAR and MAR pMET-pIRIR procedures. The L_x/T_1, L_x/T_2 and T_1/T_2 data are shown for the MAR procedure in (a) and (c), and the L_x/T_x, L_x and T_x data obtained using the SAR procedure are presented in all three panels. The dashed lines in each panel denote a 'plateau' of D_e values at about 320 Gy (a), 940 Gy (b) and 1100 Gy (c) for stimulation temperatures above 200 °C. The D_e plateau was calculated as the weighted mean of the D_e values for the SAR L_x and MAR L_x/T_2 signals measured at the two highest stimulation temperatures (250 and 280 °C for samples MTL-OSL-01 and -10, and 200 and 250 °C for MTL-OSL-07). For clarity, the data points are offset laterally at each stimulation temperature.

Fig. 10: Dose response curves for the (a) L_x/T_x and L_x/T_1, (b) L_x and L_x/T_2 and (c) T_x and T_1/T_2 signals measured at a stimulation temperature of 280 °C using the SAR and MAR pMET-pIRIR procedures for samples DGT-OSL-01, MTL-OSL-01 and -10. Each data point represents the mean value for 4–6 separate aliquots, and the vertical bars indicate the corresponding standard errors. Curves were fitted using a single saturating exponential function (see Fig. 3 caption) and normalised to unity at a dose of 523 Gy. The D_0 values of these fitted curves are shown in each panel and correspond to ~63% of the saturation intensity.

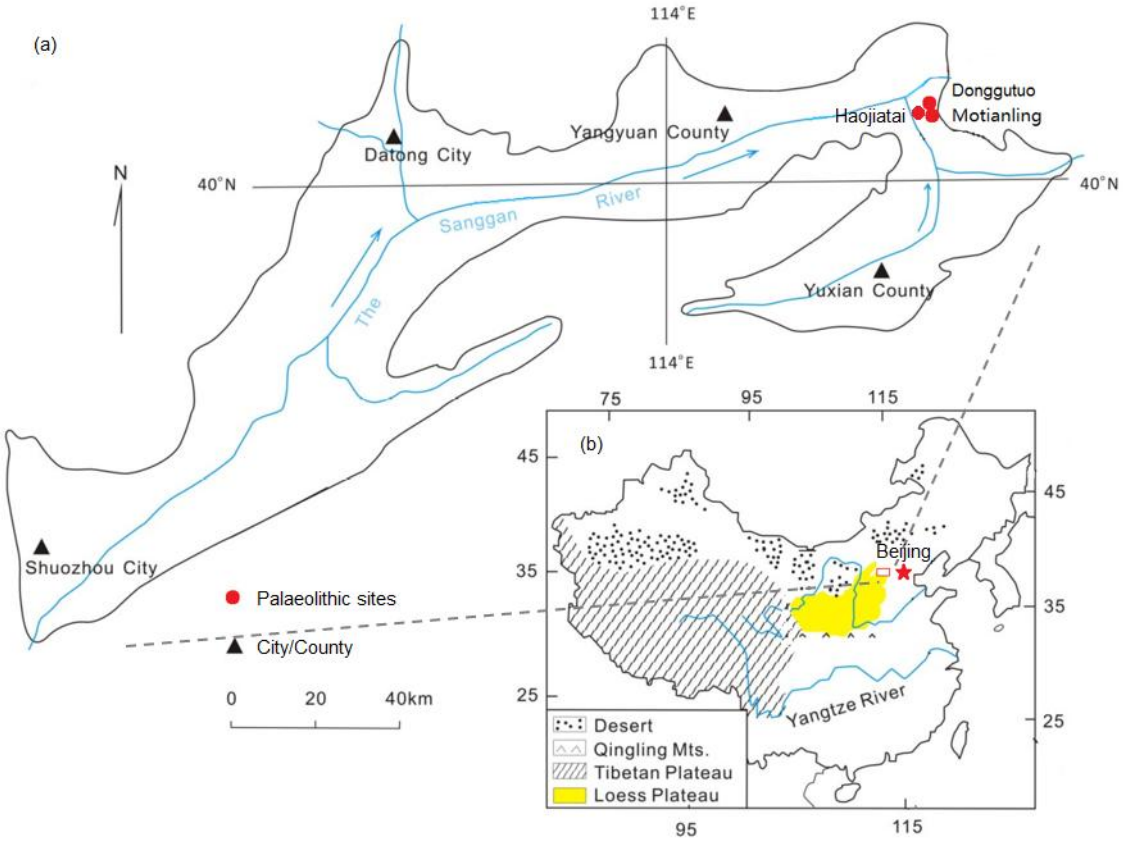
(a)
114°E
N
40°N
Datong City
Yangyuan County
Haojiatai
Donggutuo
Motianling
Sanggan River
The
Yuxian County
Shuozhou City
Palaeolithic sites
City/County
0 20 40km
(b)
75 95 115
45
35
25
Beijing
Yangtze River
Desert
Qingling Mts.
Tibetan Plateau
Loess Plateau

Fig. 1

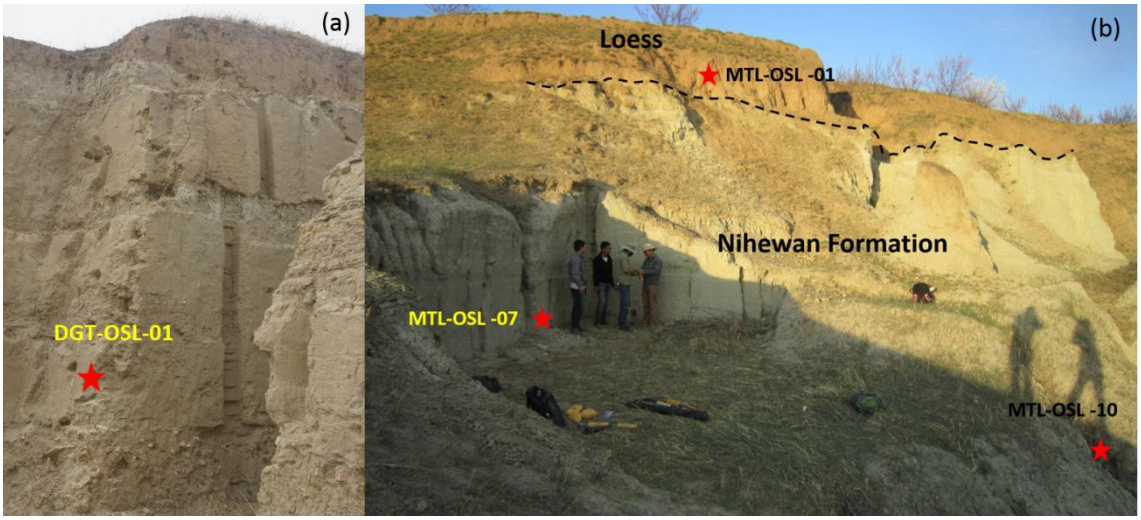

620

621 Fig. 2

622

623

624

625

626

627

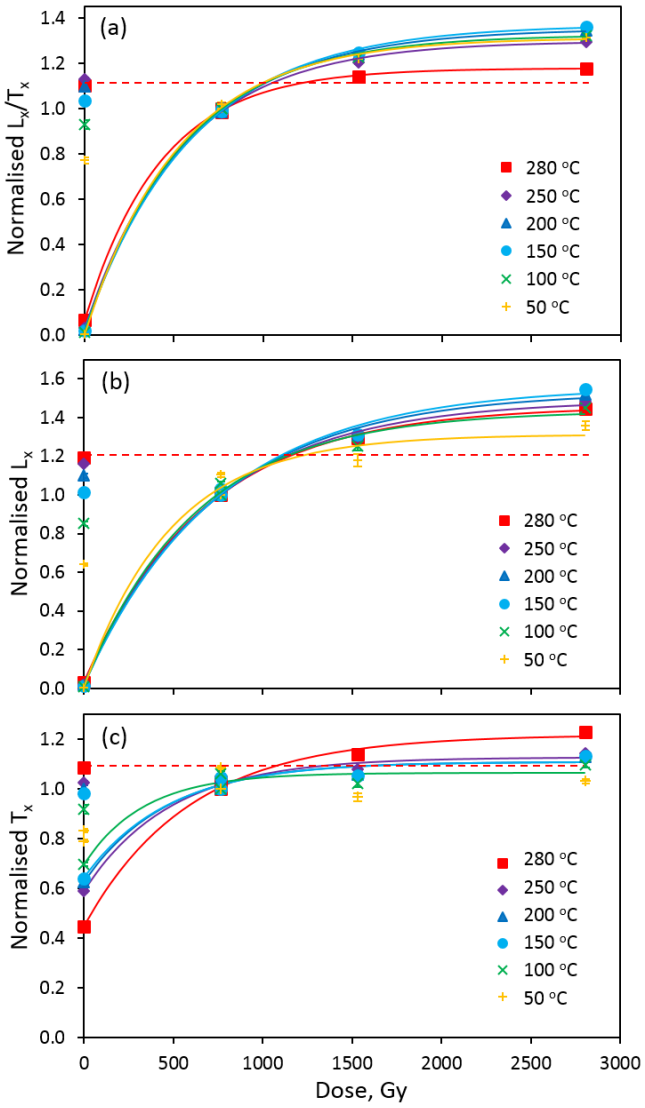

628

629

630

631 Fig. 3

632

633

634

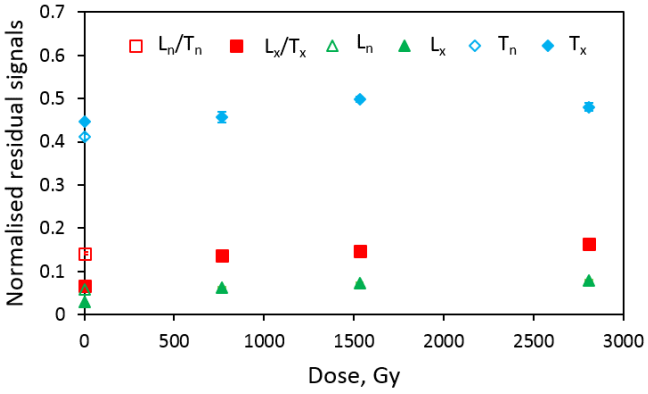

635

636

637

638 Fig. 4

639

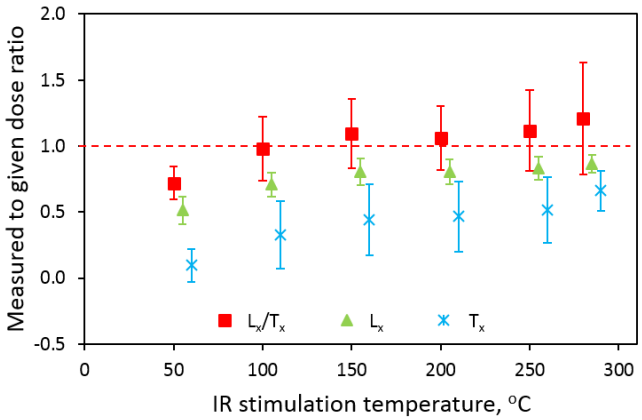
Measured to given dose ratio
2.0
1.5
1.0
0.5
0.0
-0.5
0
50
100
150
200
250
300
IR stimulation temperature, °C
Lx/Tx
Lx
Tx

Fig. 5

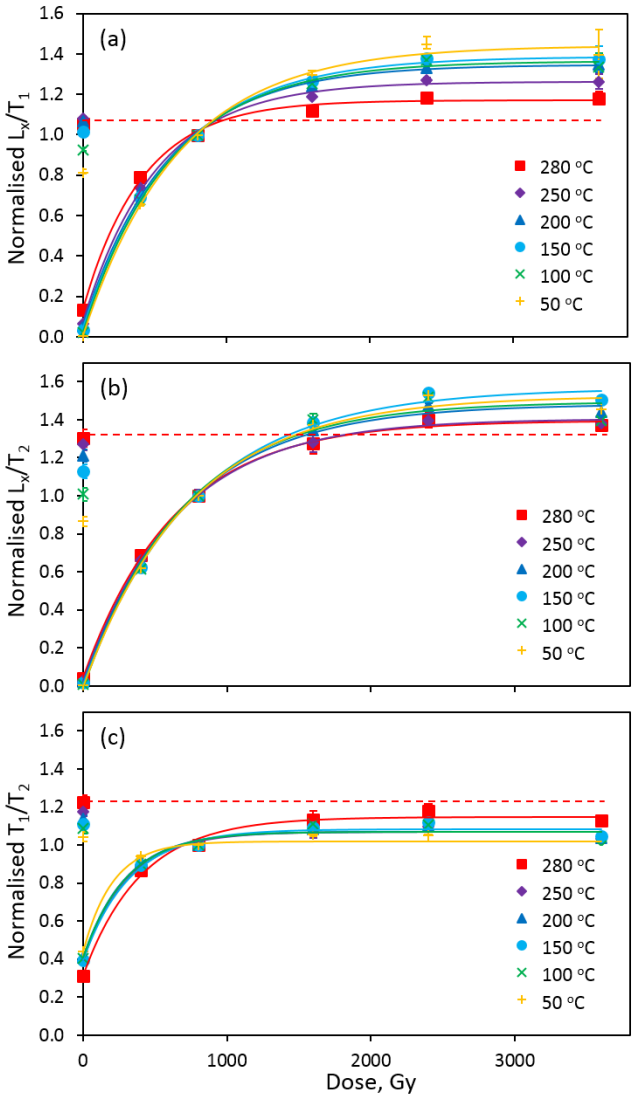
(a)
(b)
(c)
Normalised L_x/T_1
Normalised L_x/T_2
Normalised T_1/T_2
280 °C
250 °C
200 °C
150 °C
100 °C
50 °C
0.0
0.2
0.4
0.6
0.8
1.0
1.2
1.4
1.6
0
1000
2000
3000
Dose, Gy

Fig. 6

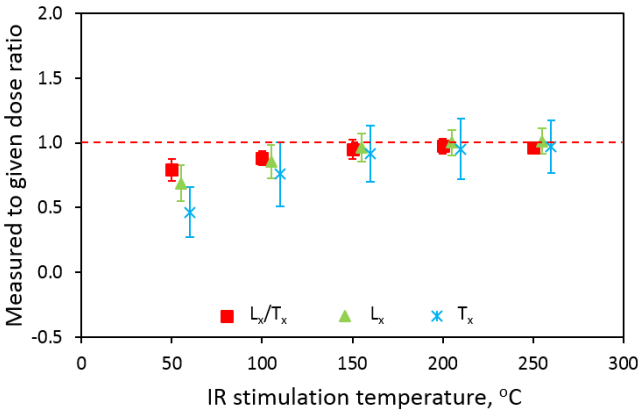
Measured to given dose ratio
2.0
1.5
1.0
0.5
0.0
-0.5
0
50
100
150
200
250
300
IR stimulation temperature, °C
Lx/Tx
Lx
Tx

Fig. 7

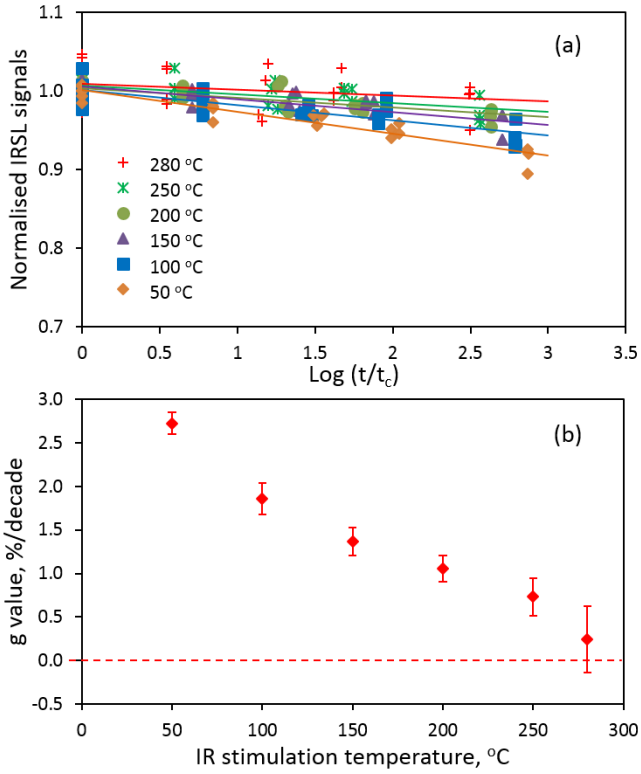
(a)
Normalised IRSL signals
280 °C
250 °C
200 °C
150 °C
100 °C
50 °C
Log (t/t$_c$)
(b)
g value, %/decade
IR stimulation temperature, °C

Fig. 8

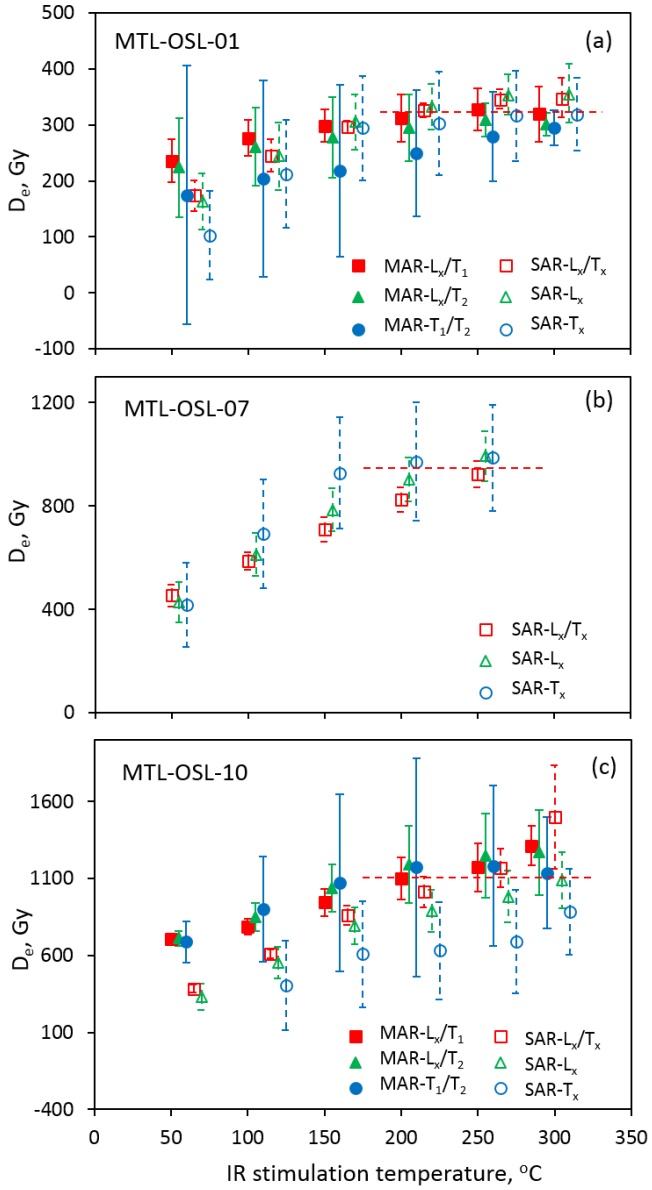
MTL-OSL-01
(a)
MTL-OSL-07
(b)
MTL-OSL-10
(c)
De, Gy
MAR-Lx/T1
MAR-Lx/T2
MAR-T1/T2
SAR-Lx/Tx
SAR-Lx
SAR-Tx
IR stimulation temperature, °C

Fig. 9

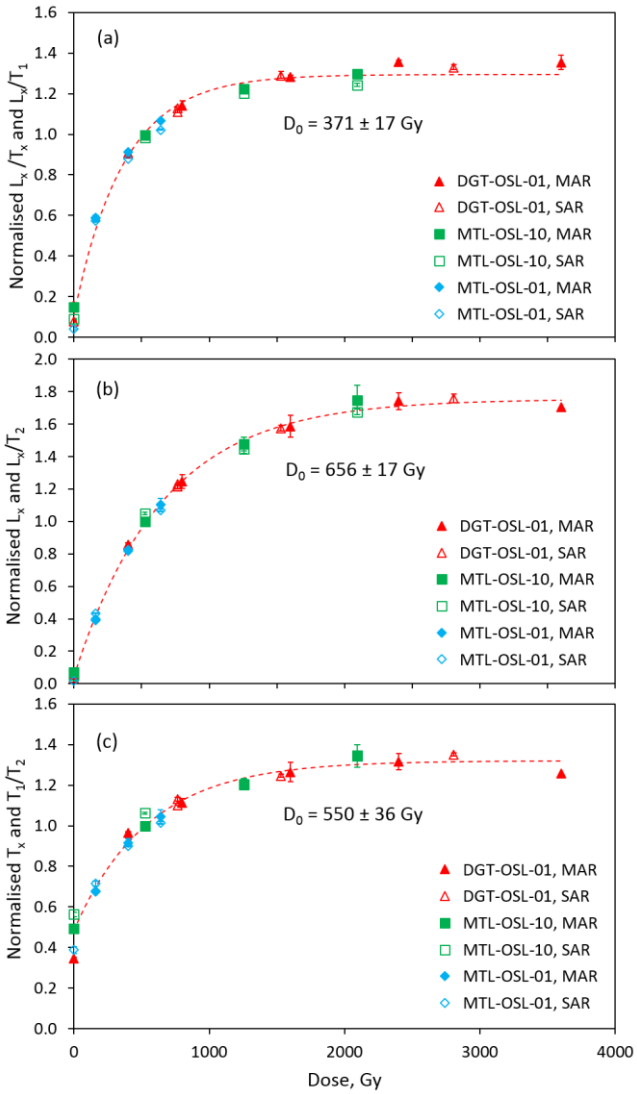
(a)
D_0 = 371 ± 17 Gy
Normalised L_x/T_x and L_x/T_1
(b)
D_0 = 656 ± 17 Gy
Normalised L_x and L_x/T_2
(c)
D_0 = 550 ± 36 Gy
Normalised T_x and T_1/T_2
DGT-OSL-01, MAR
DGT-OSL-01, SAR
MTL-OSL-10, MAR
MTL-OSL-10, SAR
MTL-OSL-01, MAR
MTL-OSL-01, SAR
Dose, Gy

Fig. 10

Table 1. Summary of the dose rate and D_e data for the samples in this study.

Sample	Location	Grain size, μm	Water content, %	U, ppm	Th, ppm	K, %	Environmental dose rate, Gy/ka					D_e, Gy [b]	Age, ka [b]
							External [a]			Internal	Total		
							Gamma	Beta	Cosmic				
DGT-OSL-01	Donggutuo	63–90	20 ± 5	2.51 ± 0.26	6.49 ± 1.00	1.88 ± 0.10	0.88 ± 0.06	1.56 ± 0.10	0.02	0.35 ± 0.03	2.80 ± 0.12	>2000 (n = 4, 6)	>700
MTL-OSL-01	Motianling	63–90	10 ± 5	3.39 ± 0.44	6.94 ± 1.16	1.40 ± 0.11	0.99 ± 0.04	1.51 ± 0.05	0.17	0.38 ± 0.03	3.05 ± 0.07	310 ± 19 (n = 6, 4)	102 ± 7
MTL-OSL-07	Motianling	63–106	20 ± 5	4.61 ± 0.74	6.09 ± 1.20	1.53 ± 0.15	1.05 ± 0.05	1.55 ± 0.08	0.08	0.41 ± 0.03	3.09 ± 0.10	994 ± 97 (n = 10)	322 ± 33
MTL-OSL-10	Motianling	63–90	20 ± 5	2.72 ± 0.38	9.70 ± 1.57	1.92 ± 0.13	1.01 ± 0.05	1.67 ± 0.08	0.07	0.38 ± 0.03	3.12 ± 0.10	1155 ± 152 (n = 4, 4)	370 ± 50

[a] Corrections for water attenuation have been made, and relative uncertainties of ± 10% were assigned to the cosmic-ray dose rates (Prescott and Hutton, 1994). The depth of sample DGT-OSL-01 is ~45 m (Xie et al., 2006), and the depths of samples MTL-OSL-01, -07 and -10 were mesured to 2.7, 9.4 and 11.2 m below modern ground surface.

[b] The final D_e values and ages for the Motianling samples are based on the weighted mean of the D_e values for the SAR L_x and MAR L_x/T_2 signals measured at the highest stimulation temperature (280 °C for samples MTL-OSL-01 and -10, and 250 °C for MTL-OSL-07). The Donggutuo sample is in field saturation, so the minimum D_e value refers to the saturation dose of the MAR L_x/T_2 signal measured at 280 °C, and the minimum age was calculated from this value divided by the environmental dose rate. The values in parentheses (n) indicate the number of aliquots used to determine the final D_e values using the SAR method (listed first) or the MAR method (the number of L_n measurements). Only the SAR procedure was applied to sample MTL-OSL-07.

Table 2. The single-aliquot regenerative-dose (SAR) procedure for pre-dose multiple elevated temperature post-infrared IRSL (pMET-pIRIR) measurements (Li et al., 2014a).

Step	Treatment	Signal
1	Give regenerative dose, D_i[a]	
2	Preheat at 320 ^{o}C for 60 s	
3	IRSL measurement at 50 ^{o}C for 100 s	$L_{x(50)}$
4	IRSL measurement at 100 ^{o}C for 100 s	$L_{x(100)}$
5	IRSL measurement at 150 ^{o}C for 100 s	$L_{x(150)}$
6	IRSL measurement at 200 ^{o}C for 100 s	$L_{x(200)}$
7	IRSL measurement at 250 ^{o}C for 100 s	$L_{x(250)}$
8	IRSL measurement at 280 ^{o}C for 100 s	$L_{x(280)}$
9	Give test dose, D_t	
10	Preheat at 320 ^{o}C for 60 s	
11	IRSL measurement at 50 ^{o}C for 100 s	$T_{x(50)}$
12	IRSL measurement at 100 ^{o}C for 100 s	$T_{x(100)}$
13	IRSL measurement at 150 ^{o}C for 100 s	$T_{x(150)}$
14	IRSL measurement at 200 ^{o}C for 100 s	$T_{x(200)}$
15	IRSL measurement at 250 ^{o}C for 100 s	$T_{x(250)}$
16	IRSL measurement at 280 ^{o}C for 100 s	$T_{x(280)}$
17	**Solar simulator bleach for 2 hr**	
18	Return to step 1	

[a] For the natural sample, i = 0 and D_i = 0 Gy. The entire sequence is repeated for several regenerative doses, including a zero dose and a repeat dose.

Table 3. The multiple-aliquot regenerative-dose (MAR) procedure for pMET-pIRIR measurements (Li et al., 2013b).

Step	Treatment	Signal
1	Give regenerative dose, D_i[a]	
2	Preheat at 320 ^{o}C for 60 s	
3	IRSL measurement at 50 ^{o}C for 100 s	$L_{x(50)}$
4	IRSL measurement at 100 ^{o}C for 100 s	$L_{x(100)}$
5	IRSL measurement at 150 ^{o}C for 100 s	$L_{x(150)}$
6	IRSL measurement at 200 ^{o}C for 100 s	$L_{x(200)}$
7	IRSL measurement at 250 ^{o}C for 100 s	$L_{x(250)}$
8	IRSL measurement at 280 ^{o}C for 100 s	$L_{x(280)}$
9	Give test dose, D_t	
10	Preheat at 320 ^{o}C for 60 s	
11	IRSL measurement at 50 ^{o}C for 100 s	$T_{1(50)}$
12	IRSL measurement at 100 ^{o}C for 100 s	$T_{1(100)}$
13	IRSL measurement at 150 ^{o}C for 100 s	$T_{1(150)}$
14	IRSL measurement at 200 ^{o}C for 100 s	$T_{1(200)}$
15	IRSL measurement at 250 ^{o}C for 100 s	$T_{1(250)}$
16	IRSL measurement at 280 ^{o}C for 100 s	$T_{1(280)}$
17	**Cut heat to 500 ^{o}C**	
18	Give test dose, D_t	
19	Preheat at 320 ^{o}C for 60 s	
20	IRSL measurement at 50 ^{o}C for 100 s	$T_{2(50)}$
21	IRSL measurement at 100 ^{o}C for 100 s	$T_{2(100)}$
22	IRSL measurement at 150 ^{o}C for 100 s	$T_{2(150)}$
23	IRSL measurement at 200 ^{o}C for 100 s	$T_{2(200)}$
24	IRSL measurement at 250 ^{o}C for 100 s	$T_{2(250)}$
25	IRSL measurement at 280 ^{o}C for 100 s	$T_{2(280)}$

[a] For the natural sample, i = 0 and D_i = 0 Gy. The entire sequence is repeated for several regenerative doses, including a zero dose and a repeat dose.